Elastic property changes in a bitumen reservoir during steam injection

Ayato Kato, University of Houston, USA
Shigenobu Onozuka, JOGMEC, Chiba, Japan
Toru Nakayama, JAPEX, Tokyo, Japan

The Hangingstone steam-assisted gravity drainage (SAGD) operation of Japan Canada Oil Sands Limited (JACOS) is approximately 50 km south-southwest of Fort McMurray in northern Alberta, Canada. JACOS started the operation in 1997 and has produced bitumen since 1999. The oil-sands reservoirs in Hangingstone occur in the Lower Cretaceous McMurray Formation and are about 300 m in depth. The sedimentary environments are fluvial to upper estuarine channel fill, and the oil-sands reservoirs correspond to vertically stacked incised valley fill with very complex vertical and horizontal distribution.

A time-lapse seismic survey was conducted to monitor the steam movement. Identical processing was used for both the 2002 baseline survey and the 2006 monitoring survey. A related article in this section by Nakayama et al. investigates differences between the data sets in the reservoir zone and shows significant difference in the seismic response around the production areas where steam was injected. Figure 1 shows seismic sections from both surveys. The large difference in the seismic response and time delay are interpreted as effects of steam injection.

We measured ultrasonic P- and S-wave velocities on core samples from the oil-sands reservoir. The oil sands are easily collapsed at room temperature due to poorly consolidated packing. The cores were frozen at the well site so that the packing was strengthened by the higher viscous bitumen. X-ray tomography (CT) images were acquired to investigate structures within the cores and detect weak portions for plugging. The oil sands are high-porous clean sands with small amounts of clay. We cut the cores into blocks and carefully whittled four plug samples from the blocks by a lathe with liquid nitrogen as the cutting fluid. The plug samples were trimmed in order to be held firmly with transducers. The four plug samples were 1.5 inches in diameter and approximately 1 inch in length (Table 1).

During the ultrasonic measurement, the plug sample was pushed into a rubber jacket and mounted by two pedestals on which P- and S-waves piezoelectric transducers were op-

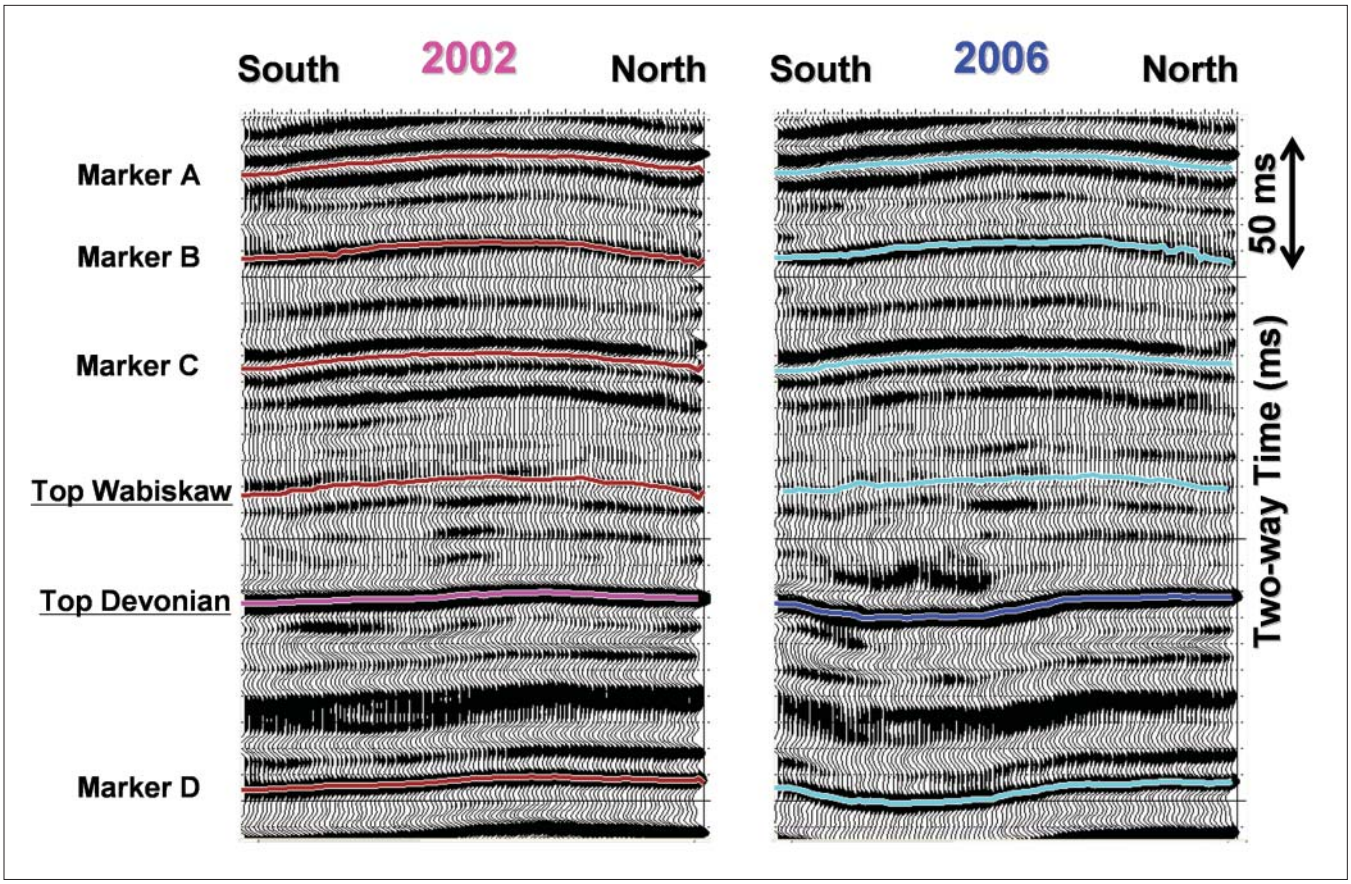

Figure 1. *Example of seismic sections with interpreted horizons. Six horizons including Top Devonian, Top Wabiskaw, and other seismic events are shown. Top Devonian is regarded as the reservoir bottom (Base McMurray), and Top Wabiskaw is about 5 m shallower than the reservoir top (Top McMurray).*

	Length (inch)	Diameter (inch)	Weight (g)	Bulk Density (g/cc)
#2	0.88	1.51	48.27	1.86
#3	1.04	1.49	56.43	1.90
#7	1.21	1.50	63.81	1.82
#10	0.89	1.49	41.99	1.65

Table 1. *List of plug samples of the oil sands.*

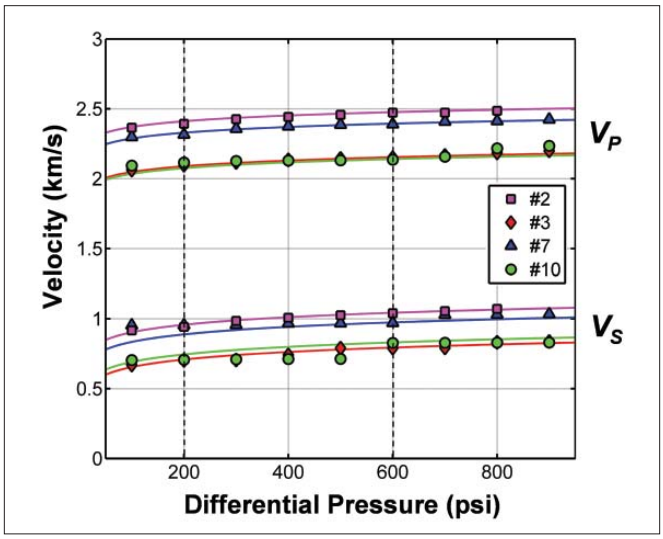

Figure 2. *P- and S-wave velocities of the oil sands as a function of differential pressure at a constant temperature of 10° C. The solid lines represent velocities calculated by Equation 1. The numbers (2, 3, 7, and 10) represent samples of the oil-sands core.*

positely attached. A unit of the two pedestals sandwiching the plug sample was loaded into a pressure vessel which can control temperature and pressure separately. P- and S-waves with 0.5-MHz frequency were propagated through the sample and recorded. Finally, the velocities were calculated from the sample length and the propagation time with correction for the system delay.

Pressure and temperature dependence

The P- and S-wave velocities in the oil sands were measured under several pressure conditions at a constant temperature of 10°C, which nearly corresponds to the reservoir temperature before the steam injection. Figure 2 shows the velocities as a function of differential pressure, i.e., confining pressure (900 psi) minus pore pressure. The P- and S-wave velocities gradually decrease with decreasing differential pressure. Using the natural logarithm as a fitting curve, we obtained a relationship between the velocities and pressure:

$$V_p = 0.0593 \cdot Log(900 - P_{pore}) - 0.375 + V_{P0}$$
$$V_S = 0.0780 \cdot Log(900 - P_{pore}) - 0.495 + V_{S0} \qquad (1)$$

P_{pore} is pore pressure (psi), V_P and V_S are P- and S-wave velocities (km/s) respectively, and V_{P0} and V_{S0} are P- and S-wave velocities (km/s) at the initial conditions (pore pressure of 300 psi and temperature of 10°C). The solid lines in Figure 2 represent the velocities calculated by Equation 1. The correla-

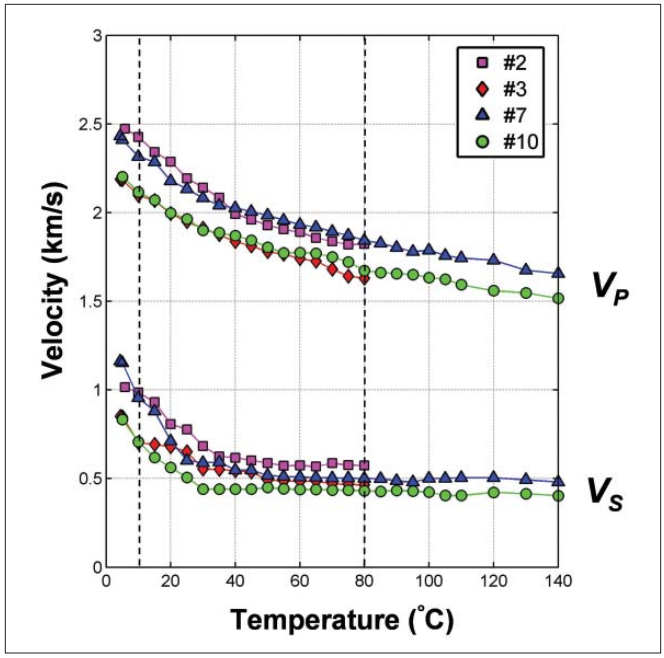

Figure 3. *P- and S-wave velocities of the oil sands as a function of temperature at pore pressure of 700 psi and confining pressure of 900 psi.*

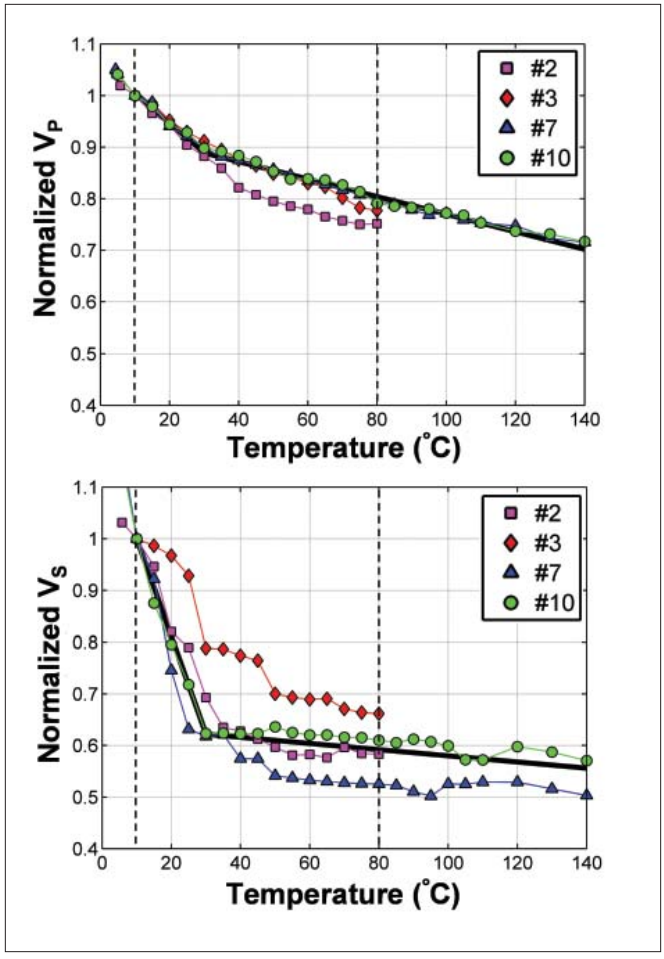

Figure 4. *Normalized P- and S-wave velocities of the oil sands as a function of temperature at pore pressure of 700 psi and confining pressure of 900 psi. Black solid lines represent Equation 2.*

tion coefficients between measured and calculated V_P and V_S are 0.99 and 0.95, respectively. The increase of pore pressure (300 to 700 psi) induced by the steam injection causes a decrease in velocity of 65 m/s for V_P and 86 m/s for V_S.

Figure 3 shows the P- and S-wave velocities as a function of temperature at a constant pore pressure of 700 psi and confining pressure of 900 psi. A slope of the velocities to temperature significantly changes at around 30°C. Whereas the P- and S-wave velocities steeply decrease at the lower temperatures, P-wave velocity more gently decreases and S-wave velocity nearly remains constant at the higher temperatures. In the lower temperature range, Han et al. (2006) pointed out that bitumen filling in the pores works as a quasi-solid to stiffen the rock grain frame moduli. We divided velocities at a given temperature by the initial velocity at 10°C to obtain normalized velocities (Figure 4). The normalized velocities were fitted with two lines which connect at 30°C.

$$\begin{aligned} &T < 30\ ^\circ C \\ &V_P / V_{P1} = -0.00550 \cdot T + 1.06 \\ &V_S / V_{S1} = -0.0190 \cdot T + 1.19 \\ &T \geq 30\ ^\circ C \\ &V_P / V_{P1} = -0.00168 \cdot T + 0.940 \\ &V_S / V_{S1} = -0.000640 \cdot T + 0.639 \end{aligned} \quad (2)$$

where T is temperature (°C), V_{P1} and V_{S1} are P- and S-wave velocities (km/s), respectively, at temperature of 10°C and pore pressure of 700 psi. The black solid lines in Figure 4 represent Equation 2. The correlation coefficients between measured and calculated V_P and V_S are 0.97 and 0.94, respectively. In accordance with Equation 2, the normalized P- and S-wave velocities at 80°C are 0.89 (V_P decrease of 11% compared to V_{P1}) and 0.62 (V_S decrease of 38% compared to V_{S1}), respectively.

Application of the Gassmann equation

Can the Gassmann equation properly predict the changes in oil-sands velocity induced by the steam injection? Or at what temperature range can it work? One implicit assumption in the Gassmann equation is that pore fluids have no rigidity. Han et al. measured ultrasonic velocities on several bitumen samples in a wide temperature range and observed that the bitumen properties are similar to conventional oils at temperatures higher than its liquid point. Dry frame moduli were calculated from the ultrasonic laboratory measurement data based on the Gassmann equation in order to investigate its validity for predicting velocity changes caused by the steam injection. In the calculation, we assumed that the pore fluids have no rigidity. Porosity and water saturation were determined to be 37% and 19.6%, respectively, by petrophysical analysis of well logs. Mineral bulk modulus was assumed to be 35.5 GPa, taking into account the small amounts of clay. Bulk modulus and density of the pore fluids were calculated by the FLAG program, which had been developed by the Fluids/DHI consortium for precisely estimating fluid properties at in-situ conditions. Figure 5 shows the calculated dry frame moduli for oil-sands sample 7 at pore pressure of 700 psi. The calculated shear modulus rapidly decreases with increasing temperature from 10 to 40°C, and then gradually decreases from 40 to 80°C. The bulk modulus obviously decreases at lower temperatures than 80°C. The significant depression of the dry frame moduli at the lower temperatures can be interpreted as: (1) the bitumen with higher viscosity stiffens the grain contacts; (2) the Gassmann equation fails because the bitumen has substantial rigidity; or (3) there is an effect of velocity dispersion between low frequency of the Gassmann

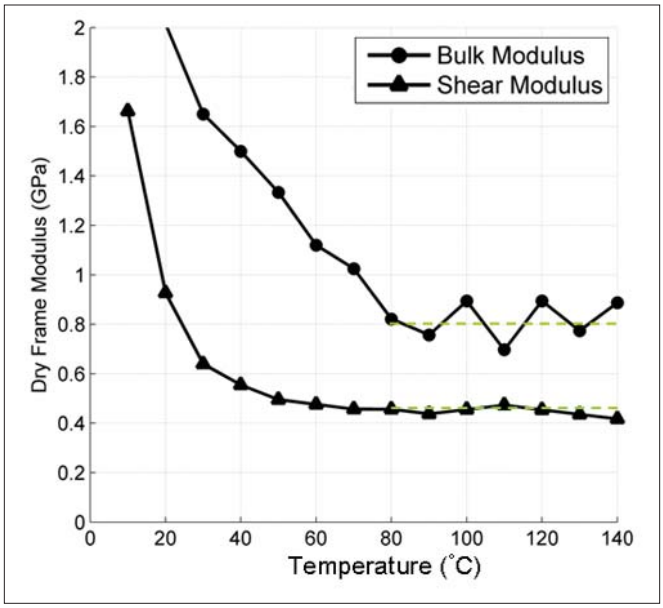

Figure 5. *Dry frame moduli of the oil sands (sample 7) at pore pressure of 700 psi, which are calculated from the ultrasonic laboratory measurements based on the Gassmann equation. Pore fluids are assumed to have no rigidity. Porosity, water saturation, and mineral bulk modulus are 37%, 19.6%, and 35.5 GPa, respectively.*

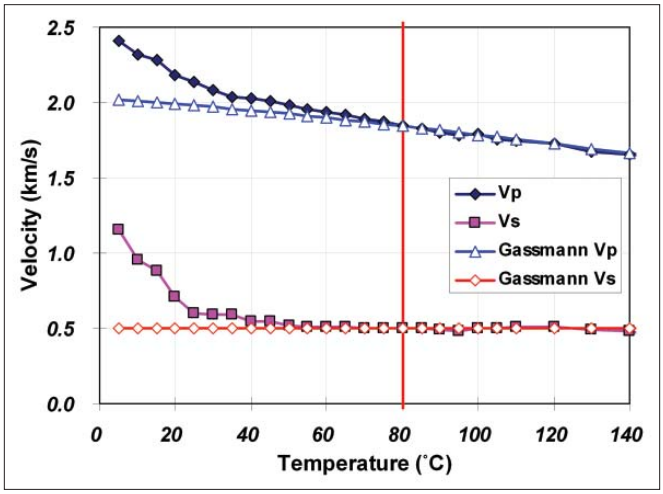

Figure 6. *Comparison between the laboratory-measured velocities and calculated velocities by the Gassmann equation for the oil sands (sample 7). Porosity, water saturation, and mineral bulk modulus in the Gassmann equation are the same as Figure 5.*

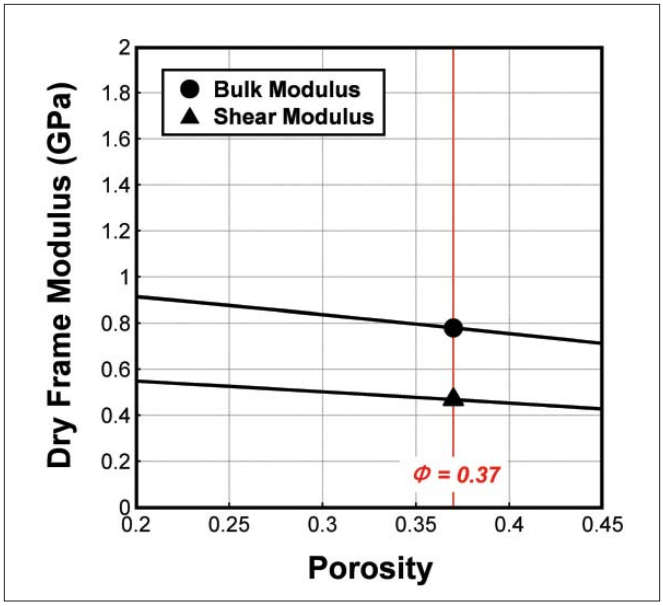

Figure 7. *Theoretical dry frame moduli at hydrostatic confining pressure of 200 psi for a poorly consolidated grain packing. They are calculated by the Walton model (ideally smooth sphere case). In the calculation, bulk and shear moduli of grain material and coordination number are assumed to be 35.6 GPa, 39.2 GPa, and 9.03, respectively.*

equation and high frequency of the ultrasonic measurement. On the other hand, the dry frame moduli do not deviate largely from one value (bulk and shear moduli are approximately 0.80 GPa and 0.46 GPa, respectively) at temperatures greater than 80°C. The unvaried dry frame moduli implies that the Gassmann equation would be applicable for predicting velocity changes at the higher temperatures at which the bitumen neither stiffens the grain contact nor has rigidity, and the velocity dispersion is small enough to be neglected.

In order to justify the above hypothesis, we calculated velocity changes caused by fluid property changes based on the Gassmann equation. In the calculation, dry frame moduli are assumed constant (even though temperature varies) and are calculated from ultrasonic laboratory measurements at 80°C based on the Gassmann equation. For a given new temperature, the original pore fluids at 80°C are assumed to be replaced by new fluids that equilibrate with the new temperature. Figure 6 compares measured and calculated velocities. The calculations are fairly consistent with the measurements at temperatures higher than 80°C. This result encourages the use of the Gassmann equation for predicting velocity changes caused by any property changes in pore fluid (due to temperature changes and also water saturation and phase changes) at the higher temperatures until the rock frame undergoes direct damage from the steam injection.

The dry rock frame is considered to have poorly consolidated grain packing. Thus, we calculated the theoretical dry frame moduli for an idealized spherical random grain packing and compared them with the calculated values by the Gassmann equation. In the theoretical calculation, the ideally smooth sphere case of the Walton model (Walton, 1987) was applied. Bulk and shear moduli of the grain material were assumed to be 35.6 GPa and 39.2 GPa, respectively. Porosity and average number of contacts per grain (coordination number) were assumed to be 37% and 9.03, respectively. Figure 7 shows the dry frame moduli at hydrostatic confining pressure of 200 psi. The dry frame bulk and shear moduli at 37% porosity are 0.78 GPa and 0.47 GPa, respectively, and nearly consistent with the dry frame moduli at greater temperatures than 80°C calculated by the Gassmann equation.

Sequential rock physics model

We combined the laboratory measurement results to obtain a sequential rock physics model that can predict sequential velocity changes induced by the steam injection:

1. P_{pore} 300 psi → 700 psi (at $T = 10°C$)

$$V_P = 0.0593 \cdot Log(900 - P_{pore}) - 0.375 + V_{P0}$$
$$V_S = 0.0780 \cdot Log(900 - P_{pore}) - 0.495 + V_{S0} \quad (3\text{-}1)$$

2. T 10°C → 30°C (at $P_{pore} = 700$ psi)

$$V_p = (-0.00550 \cdot T + 1.06)V_{P1}$$
$$V_S = (-0.0190 \cdot T + 1.19)V_{S1} \quad (3\text{-}2)$$

3. T 30°C → 80°C (at $P_{pore} = 700$ psi)

$$V_p = (-0.00168 \cdot T + 0.940)V_{P1}$$
$$V_S = (-0.000640 \cdot T + 0.639)V_{S1} \quad (3\text{-}3)$$

4. $T \geq 80°C$ (at $P_{pore} = 700$ psi)
The Gassmann equation can predict velocity changes. Fluid properties are based on the FLAG program. (3-4)

V_{P1} and V_{S1} are P- and S-wave velocities (km/s), respectively, at pore pressure of 700 psi and temperature of 10°C, and can be calculated from the first relations between the velocities and pressure (Equation 3-1). Once steam is injected into the reservoir, the pressure front rapidly spreads to the periphery, and the temperature front follows it. The P- and S-wave velocities decrease due to the pore-pressure increase in a natural logarithm relationship with differential pressure (Equation 3-1). After the pressure change, the velocities decrease with increasing temperature as a linear relation with a change in the slope at 30°C as shown in Figure 4 (Equations 3-2 and 3-3). The velocities at temperatures greater than 80°C can be calculated via the Gassmann equation with the FLAG program (Equation 3-4).

Velocity dispersion

Significant frequency differences exist between ultrasonic laboratory measurements and surface seismic. Schmitt (1999) showed that sonic velocities in the heavy-oil zone are much higher than surface seismic frequency velocities collected by VSP. We also observed significant velocity dispersion in this field (Figure 8). The seismic interval velocities were calculated from two-way time differences between two seismic horizons (Top Wabiskaw and Top Devonian in Figure 1) at well locations which nearly correspond to the reservoir top and bottom. The sonic interval velocities were calculated from

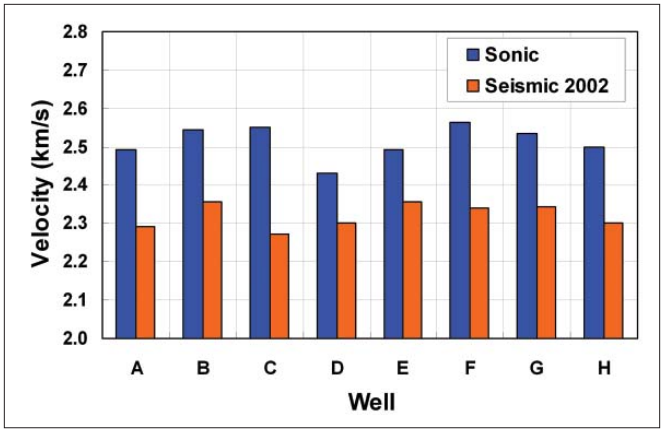

Figure 8. *Interval velocity of the oil-sands reservoir at well locations from the surface seismic and the sonic log data. The seismic interval velocities were calculated from two-way time differences between two seismic horizons which nearly correspond to the reservoir top and bottom. The sonic interval velocities were calculated from time-depth relations of the corresponding reservoir interval. Letters A–H represent wells used for the calculation.*

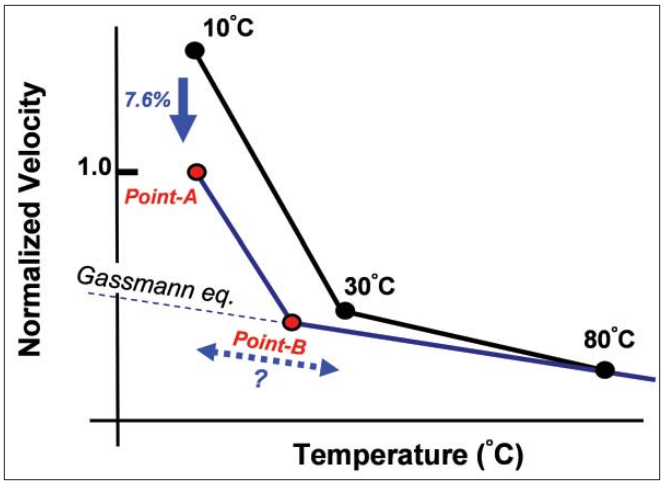

Figure 9. *Illustration of a practical method for calibrating the velocity dispersion. Point B represents temperature limitation of the Gassmann equation for the low-frequency band of surface seismic. Point A represents surface seismic velocity at initial conditions which are calculated from well sonic velocity with the average velocity dispersion. Point A and Point B are transformed into normalized velocity and connected with each other by a line.*

time-depth relations of the corresponding reservoir interval. The interval velocities were not affected by the steam injection because the surface seismic and well-log data used for the calculation were acquired prior to it. Figure 8 shows that the seismic velocities are lower than the sonic velocities. For the eight wells calculated, the interval velocity difference is 7.6% on average.

We propose a practical method for calibrating the velocity dispersion (Figure 9). As stated before, the Gassmann equation is applicable at temperatures greater than 80°C for high-frequency ultrasonic laboratory measurements. When we apply the Gassmann equation to the surface seismic data, we assume that the temperature limitation of the Gassmann equation can extend to lower temperature until the dry frame moduli change or the bitumen has substantial rigidity. In addition, we have the average value of the interval velocity difference between the surface seismic and the sonic data at the initial condition. The seismic velocity at the initial condition is estimated from the sonic velocity with the average velocity dispersion. We transform them into normalized velocities and connect the initial point (Point A) with the temperature limitation of the Gassmann equation (Point B) by a line in fashion similar to Figure 4. However, we do not know the temperature limitation of the Gassmann equation. Fortunately, Point B can only move in a small range from 10 to 30°C. Assuming the temperature limitation is 25°C, we modified the coefficients associated with the temperature dependence in Equation 3 and obtained a new sequential rock physics model which is adapted for the low-frequency band of the surface seismic.

1. P_{pore} 300 psi → 700 psi (at $T = 10^{\circ}C$)

$$V_P = 0.0593 \cdot Log(900 - P_{pore}) - 0.375 + V_{P0} \quad (4\text{-}1)$$
$$V_S = 0.0780 \cdot Log(900 - P_{pore}) - 0.495 + V_{S0}$$

2. T 10°C → 25°C (at $P_{pore} = 700$ psi)

$$V_P = (-0.00433 \cdot T + 1.04)V_{P1} \quad (4\text{-}2)$$
$$V_S = (-0.0239 \cdot T + 1.24)V_{S1}$$

3. $T \geq 25^{\circ}C$ (at $P_{pore} = 700$ psi) (4-3)
The Gassmann equation can predict velocity changes. Fluid properties are based on the FLAG program.

Sequential elastic property changes

To understand elastic property changes of the oil-sand reservoir during the steam injection, we represented the sequential reservoir conditions using 23 steps (Figure 10). Pore-pressure changes occur in steps 1-5 and temperature in steps 5-23. In addition, adjacent to the injector well, the movable bitumen is largely replaced by hot water at step 18 and water phase changes from liquid to steam at step 21.

Step 1-5:	*pore pressure increases (from 300 to 700 psi)*
Step 5-23:	*temperature increases (from 10 to 300°C)*
Step 18:	*bitumen is replaced by hot water at 200°C (Sw from 20 to 80%)*
Step 21:	*phase changes from hot water to steam at 260°C*

Assuming that the sonic P- and S-wave velocities at the initial condition (step 0) are 2.4 km/s and 1.0 km/s, respectively, the seismic velocities (step 1) are calculated from the sonic velocities with the average velocity dispersion. The P- and S-wave velocities slightly decrease during the pressure changes from step 1 to 5. In the temperature increase from step 5 to 8, the P- and S-wave velocities decrease and the V_P/V_S ratio significantly increases because the amount of decrease of the S-wave velocity is relatively larger than the P-wave velocity. After step 8 (25°C), the P-wave velocity continues to

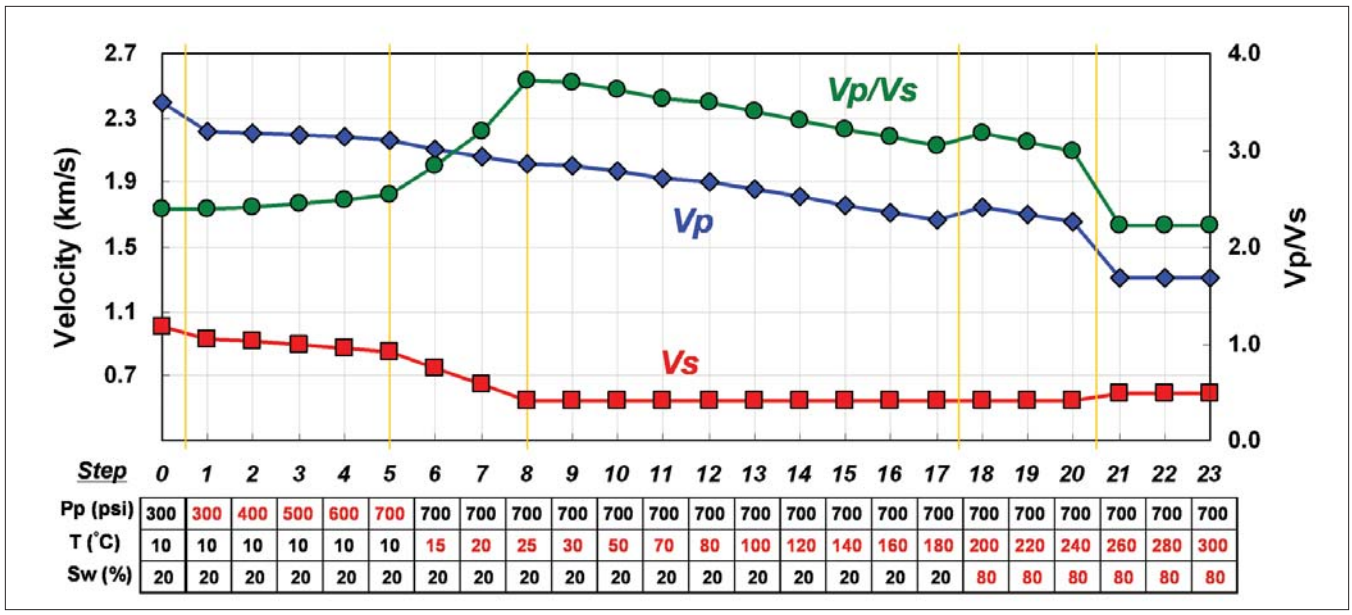

Figure 10. *Sequential P- and S- wave velocities and V_P/V_S ratio changes induced by steam injection. Sequential reservoir condition changes are represented by 23 steps. Pore-pressure changes occur from step 1 to 5, and temperature changes from step 5 to 23. In addition, adjacent to the injector well, the movable bitumen is largely replaced by hot water at step 18 and water phase changes from liquid to steam at step 21. The sonic P- and S-wave velocities at the initial condition (step 0) are assumed to be 2.4 km/s and 1.0 km/s, respectively.*

decrease until step 18 while the S-wave velocity is virtually constant (because the shear modulus is constant). At step 18 (200°C), where the movable bitumen is largely replaced by the hot water (SW from 20% to 80%), the P-wave velocity slightly increases because the hot water has a faster P-wave velocity than the bitumen. Finally, the water phase changes from liquid to steam at step 21 (260°C), leading to significant P-wave velocity drop (while the S-wave velocity slightly increases because of density decrease).

Other elastic property changes of the oil sands can be calculated from the velocity and density changes. The velocity changes can be calculated by the rock physics model (Equation 4), and density changes can be calculated by the FLAG program. Figure 11 shows examples of the sequential elastic property changes based on the conditions of Figure 10. With increasing pore pressure (step 1-5), acoustic impedance and $\mu\rho$ slightly decrease, and V_P/V_S ratio slightly increases while $\lambda\rho$ is virtually constant. The temperature increase from 10 to 25°C (step 5-8) causes significant change in V_P/V_S ratio (increase) and $\mu\rho$ (decrease). At higher temperatures than 25°C, acoustic impedance, V_P/V_S ratio, and $\lambda\rho$ decrease, except in steps 18 through 20, while $\mu\rho$ is virtually constant. The water phase change from hot water to steam causes significant decrease in acoustic impedance, V_P/V_S ratio, and $\lambda\rho$.

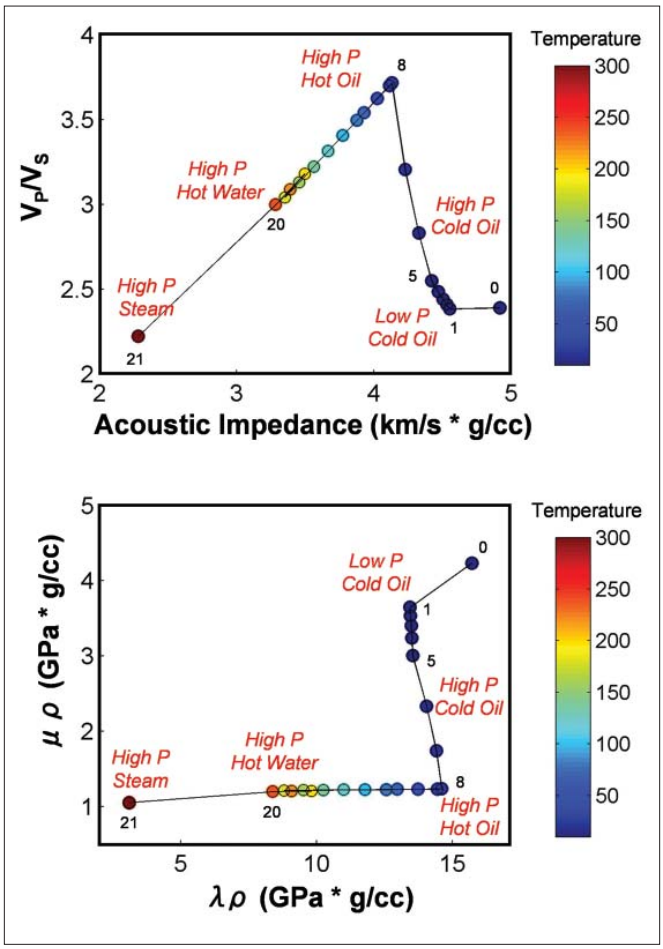

Figure 11. *Sequential elastic property changes induced by the steam injection based on the reservoir conditions of Figure 10. (top) Crossplot between acoustic impedance and V_P/V_S ratio. (bottom) Crossplot between $\lambda\rho$ and $\mu\rho$. Numbers in the crossplots represent the step in Figure 10.*

Conclusions

We measured and analyzed the ultrasonic velocities of the oil-sands cores acquired from the SAGD operations and constructed the sequential rock physics model. The practical method for calibrating the velocity dispersion was proposed, and the sequential model was modified to be adapted for the low-frequency band of the surface seismic. We predicted elastic property changes induced by the steam injec-

tion. The S-wave velocity can be useful for distinguishing a gently-warmed area front because it significantly decreases at around 20°C. The V_P/V_S more dramatically changes with the reservoir condition change. The V_P/V_S significantly increases at the gently-warmed area front, and then significantly drops at the steam front.

Suggested reading. "Heavy oils—seismic properties" by Batzle et al. (*TLE*, 2006). "Heavy oils: Their shear story" by Behura et al. (GEOPHYSICS, 2007). "Monitoring an oil-sands reservoir in northwest Alberta using time-lapse 3D seismic and 3D P-SV converted-wave data" by Nakayama et al. (*TLE*, 2008). "Acoustic property of heavy oil-measured data" by Han et al. (SEG 2006 *Expanded Abstracts*). "The effective elastic moduli of a random packing of spheres" by Walton (*Journal of the Mechanics and Physics of Solids*, 1987). "Seismic attributes for monitoring of a shallow heated heavy oil reservoir: A case study" by Schmitt (GEOPHYSICS, 1999). TLE

Acknowledgments: This study was conducted as a joint project between Japan Canada Oil Sands Limited (JACOS) and Japan Oil, Gas and Metals National Corporation (JOGMEC). The authors thank Japan Petroleum Exploration Company Limited (JAPEX), JACOS and JOGMEC for permission to publish these data.

Corresponding author: akato@mail.uh.edu